ORIGINAL RESEARCH

Circular RNA circLRCH3 Inhibits Proliferation, Migration, and Invasion of Colorectal Cancer Cells Through miRNA-223/LPP Axis

Yiming Yang, Di Wang, Kaixiong Tao, Guobin Wang

Department of Gastrointestinal Surgery, Union Hospital, Tongji Medical College, Huazhong University of Science and Technology, Wuhan, 430033, People's Republic of China

Correspondence: Guobin Wang, Email wgb@hust.edu.cn

Purpose: Colorectal cancer (CRC) is one of the most common carcinomas worldwide with a high mortality rate. Numerous studies suggest that circular RNA (circRNA) plays a crucial role in the progression of various carcinomas, including CRC. The present work focused on exploring the role and underlying molecular mechanism of action of the circRNA circLRCH3 in CRC.

Methods: Real-time reverse transcription-quantitative polymerase chain reaction (RT-qPCR) was conducted to detect expression levels of circLRCH3, miR-233, and lipoma preferred partner (LPP). The 3-(4,5-dimethylthiazol-2-yl)-2,5-diphenyltetrazolium bromide (MTT) assay was used to measure the proliferation of CRC cells and the transwell assay was used to evaluate cell migration and invasion capacity. A flow cytometry assay was used to analyze the effect of circLRCH3 on the distribution of the cell cycle and apoptosis of CRC cells. The expression of LPP was analyzed using Western blotting or an RT-qPCR assay. The relationship between miR-223 and circLRCH3, and that between miR-223 and LPP, was predicted and examined using bioinformatics analysis and luciferase reporter gene experiments. A xenograft tumor formation assay was also performed.

Results: We found that the expression level of circLRCH3 was downregulated in CRC cells and negatively correlated with miR-223. The overexpression of circLRCH3 or silencing of miR-223 inhibited the growth, invasion, and migration of CRC cells, but promoted their apoptosis. In contrast, overexpression of miR-223 and depletion of LPP severally abrogated the tumor suppressive roles of circLRCH3 and miR-223 knockdown in CRC cells in vitro. The xenograft experiments in nude mice also proved the antitumor effect of circLRCH3.

Conclusion: These results suggested that the circLRCH3/miR-223/LPP axis likely plays a critical role in CRC.

Keywords: circLRCH3, miR-223, LPP, colorectal cancer, TCGA, GEO

Introduction

Colorectal cancer (CRC) is one of the most prevalent causes of cancer-related morbidity and mortality worldwide.[1–3] Despite numerous therapeutic approaches and novel clinical therapies were employed, the overall survival rate remained poor due to late diagnosis and cancer metastasis.[4,5] Elucidation of the latent developmental mechanism of CRC may enhanced the understanding of the complicated pathogenesis and provide new methods for more effective treatments.

Circular RNAs (circRNAs), a group of novel non-coding RNA transcripts characterized by closed continuous loops stably existing in tissues and cells, have been identified in back-splicing precursor mRNA.[6] These circRNAs are characterized by a "head to tail" splicing structure, and dysregulated circRNAs have been reported to play important roles in almost all types of cancers.[7,8] Previous studies have shown that circRNAs play multiple important roles in cellular physiology through their actions as microRNA (miRNA) sponges, RBP-binding molecules, transcriptional regulators, or templates for protein translation. For example, circMRPS35 regulates phosphatase and tensin homolog (PTEN) stability through the circMRPS35-miR-148a-STX3 axis in hepatocellular carcinoma (HCC) cells.[9] Yang et al reported that circ-CTNNB1 promotes β-catenin signaling and cancer progression via DDX3-mediated transactivation of

YY1.[10] Gao et al demonstrated that Circular RNA-encoded oncogenic E-cadherin variant promotes glioblastoma development through activation of EGFR–STAT3 signaling.[11] Due to the relatively stable characteristics of circRNA and its important role in the tumorigenicity of CRC, circRNA can serve as a new diagnostic marker and therapeutic target for CRC.

MicroRNAs (miRNAs) are a group of endogenous, conserved, noncoding RNAs, typically 18–25 nucleotides long that can regulate numerous biological processes including cell proliferation, migration, differentiation, and apoptosis.[12,13] Furthermore, miRNAs have been shown to decrease the expression of various genes via partial base-pairing to the target mRNA of the target gene 3′ untranslated region (3′UTR).[14] Recently, MiR-223 has been demonstrated to be regulated by lncRNA or circRNA via ceRNA crosstalk among diverse cancers.[15,16] However, the regulatory relationship between circRNA and miR-223 has not been reported yet. Lipoma preferred partner (LPP) is a LIM domain protein, which has multiple functions as an actin-binding protein and a transcriptional coactivator, and it has been suggested that LPP has some roles in cell migration or invasion,[17] whereas its role in CRC development and its relationship with circLRCH3 and miR-223 are largely unknown.

In the present study, we aimed to explore the expression and function of circLRCH3 and its underlying mechanisms in CRC. Our study confirmed, to the best of our knowledge, for the first time that the circLRCH3/miR-223/LPP axis participates in CRC progression. These findings provide a novel and potentially effective method for CRC diagnosis and treatment and we hypothesized that circLRCH3 affects OS cell proliferation, migration, and invasion via the miR-223/LPP axis.

Materials and Methods
Bioinformatics Data Mining
For the bioinformatics data mining, the raw CRC circRNA (GSE172229 and GSE138589), miRNA (the Cancer Genome Atlas [TCGA]-colon adenocarcinoma [COAD] and TCGA-READ), and mRNA data (TCGA-COAD and TCGA-READ) with their corresponding clinical information were first downloaded from Gene Expression Omnibus (GEO) and TCGA database. Next, the expression matrix was used for normalization based on the Robust Multi-Array Average (RMA) and Linear Models for Microarray (LIMMA) algorithm.[18]

Then, the differentially expressed circRNAs/miRNAs/mRNAs (DECs/DEMs/DEGs) between the CRC samples and the non-tumor samples were screened out using DESeq2 package.[19] The inclusion criteria were set as $P < 0.05$ and logFC > 1.3. Then, the overlapping analysis was performed to identify candidate molecules based on differentially expressed genes (DEGs) and predicted targets. Subsequently, the overlapped molecules were visualized using the VennDiagram package.

Furthermore, the volcano map was constructed using the ggplot package to measure the expression level of the selected DEGs between the CRC samples and the normal samples. We collected 46 CRC and para-tumor tissues from the Union Hospital affiliated to the Tongji Medical College of Huazhong University of Science and Technology, Wuhan, China. The histopathological reports confirmed the CRC diagnosis. All procedures were undertaken in accordance with guidelines set forth by the Declaration of Helsinki. All patients signed the informed consent forms before participating and the protocols were approved by the ethics committee of the Huazhong University of Science and Technology.

Bioinformatic Prediction
Circbase[20] was used to retrieve the biological information on circLRCH3, whereas circRNA Interactome (CRI) was used to predict the circLRCH3-binding microRNAs and the binding sites.[21] MiRWalk2.0[22] was used to investigate the predicted and validated target genes of miR-223. A target gene that was predicted simultaneously using the following four algorithms, miRWalk2.0,[22] TargetScan6.2,[23] miRanda,[24] and RNA22[25] was adopted for the subsequent analysis. Then, the overlapping genes analysis was performed on the predicted target genes, validated targets, and DEGs from the TCGA-READ and TCGA-COAD datasets. The DEGs between the CRC and the normal samples were identified using the screening methods mentioned in this section.[19]

Cell Culture and Transfection

The human CRC SW480, LoVo, DLD-1, SW620, HCT-116, and normal colonic epithelial cell line (NCM460) were obtained from the American Type Culture Collection (ATCC, Manassas, VA, USA). The cells were cultured in Dulbecco's modified Eagle's medium (DMEM, Invitrogen, Carlsbad, CA, USA) containing with 10% dialyzed fetal bovine serum (FBS, Gibco Life Technologies), and with 1% penicillin and streptomycin at 37°C in the presence of 5% carbon dioxide.

The miR-223 mimic and corresponding mimic negative control (miR-NC) were designed by GenePharma (Shanghai, China). The pcDNA (Vector) and pcDNA-LPP overexpression (LPP-OE) plasmids were obtained from GenePharma (Shanghai, China). The target cells were transfected with the mimic, plasmids, and miR-NC using the Lipofectamine 2000 transfection reagent (Invitrogen) according to the manufacturer's instruction.

Reverse Transcription-Quantitative Polymerase Chain Reaction (RT-qPCR)

We employed TRIzol reagent (Invitrogen, Carlsbad, CA, USA) to extract the total RNA from CRC cells based on the manufacturer's protocol. Rt was conducted using the PrimeScript^{TM} RT Master Mix (Takara, Japan). The real-time qPCR was performed using a RealMasterMix kit (Tiangen Biotech) according to the manufacturer's protocol. The circRNA, miRNA, and mRNA levels were normalized to U6 or glyceraldehyde 3-phosphate dehydrogenase (GAPDH) and was quantified using the $2^{-\Delta\Delta Ct}$ method. All experiments were performed at least three times. The specific primer sequence is shown in Table 1.

Table 1 The Sequence of PCR Primers and Oligonucleotide Sets Used for Short Hairpin RNAs, or Probe

Primer	Sequence
MiR-223	Forward: 5'-CAGCACCACTGAATCACAGA-3'
	Reverse: 5'-GTGCAGGGTCCGAGGT-3'
U6	Forward: 5'-TGCGGGTGCTCGCTTCGGCAGC-3'
	Reverse: 5'-CCAGTGCAGGGTCCGAGGT-3'
MiR-431	Forward: 5'-ACACACTTCGGGTTTCACGA-3'
	Reverse: 5'-AAGTCCCTTCGTCTCCCTCA-3'
GAPDH	Forward: 5'-CAAGTATGATGACATCAAG-AAGGTGG-3'
	Reverse: 5'-GGAAGAGTGGGAGTTGCTGTTG-3'
SSPN	Forward: 5'-TGCTAGTCAGAGATACTCCGTTC-3'
	Reverse: 5'-GTCCTCTCGTCAACTTGGTATG-3'
BVES	Forward: 5'-GGACGGAGTGGGCGATATC-3'
	Reverse: 5'-CCTCGAACCGCGCAAA-3'
HACE1	Forward: 5'-GAGAGAGCGATGGAGCAACT-3'
	Reverse: 5'-ACAGCAAAACCAAGCATTCC-3'
LPP	Forward: 5'-GTGCAATGTGTGTTCCAAGC-3'
	Reverse: 5'-TGGCATAATAGGCTCCTTGC-3'
PRDM1	Forward: 5'-TAAAGCAACCGAGCACTGAGA-3'
	Reverse: 5'-ACGGTAGAGGTCCTTTCCTTTG-3''
CircLRCH3 (convergent)	Forward: 5'-AGGGCAGAAACCAACAAAG-3'
	Reverse: 5'-ACAGATCGAGGTCGCACAT-3
CircLRCH3 (divergent)	Forward: 5'-GACGGTGTTGTTCTTTGCC-3'
	Reverse: 5'-TTGTTGGTTTCTGCCCTGA-3
sh-Scb	5'-CCGGGCGAACGATCGAGTAAACGGACTCGAGTCCGTTTACTCGATCGTTCGCTTTTT-3' (sense);
	5'-AATTCAAAAAGCGAACGATCGAGTAAACGGACTCGAGTCCGTTTACTCGATCGTTCGC-3' (antisense)
sh-LPP	5'-CCGGGGCTCCAGTGGAGAGTTCTTACTCGAGTAAGAACTCTCCACTGGAGCCTTTTTG-3' (sense);
	5'-AATTCAAAAAGGCTCCAGTGGAGAGTTCTTACTCGAGTAAGAACTCTCCACTGGAGCC-3' (antisense)
circLRCH3 (probe)	AGGTCTGTCATCACTTACAGCTGGTGAGGG (antisense)
	CCCTCACCAGCTGTAAGTGATGACAGACCT (sense)

Western Blot Assay

Radioimmunoassay precipitation assay (RIPA) buffer was used to extract the total proteins of target cells according to the manufacturer's protocols. The protein concentration was measured using the bicinchoninic acid (BCA) assay (Pierce, Rockford, IL, USA). The total protein was separated using 10% sodium dodecyl sulfate (SDS) polyacrylamide gel electrophoresis and then transferred onto polyvinylidene fluoride (PVDF) membranes (Invitrogen). Membranes were then probed overnight at 4°C with GAPDH (1:5000, ab8245) and LPP (1:10000, ab126608) antibodies followed by incubation with secondary antibodies at room temperature for 1 h. The signals were visualized using LICOR Odyssey system (LI-COR, NE, USA) with enhanced chemiluminescent (ECL) reagents.

Luciferase Reporter Assay

The CRC cells were placed in 24-well plates at a density of 1×10^4/well. The next day, the CRC cells were co-transfected with 100 ng pMIR-REPORT luciferase vector consisting of a wild-type (WT) or mutated (MUT) LPP 3′UTR and the miR-223 mimic or miR-NC using the Lipofectamine 2000 transfection reagent for the 3′-UTR reporter activity assay. The transfection was conducted according to the manufacturer's instructions. After incubation for 2 days, the CRC cells were collected and the luciferase assays were performed using the Dual Luciferase Reporter assay system (Promega).

Transwell Assay

The invasion and migration capacity of the CRC cells was measured using a Transwell assay. Briefly, transfected CRC cells (5×10^3/well) were placed in the upper chamber of the Transwell system with serum-free growth medium and the lower compartment was filled with 500 μL culture medium containing 30% FBS. After a 24 h incubation, the chambers were washed twice with PBS, the cells were fixed using 4% paraformaldehyde, and then stained with 0.1% crystal violet. Finally, the stained cells were counted using a microscope.

Cell Proliferation Assay

The proliferative ability of the cells was assessed using a 3-(4,5-dimethylthiazol-2-yl)-2,5-diphenyltetrazolium bromide (MTT) assay according to the manufacturer's instructions. Briefly, cells were placed in a 96-well plate at a density of 5×10^3 cells/well and incubated for 1 to 5 days at 37 °C. Then, 20 μL MTT solution was added to each well, followed by incubation at 37°C for 4 h, and then 150 μL dimethyl sulfoxide (DMSO) was added after removing the supernatant. Finally, the absorbance at 490 nm was measured using a microplate reader and the cell proliferation ability was measured using a 5-ethynyl-2 -deoxyuridine (EdU) assay kit (Beyotime, Shanghai, China).

Wound Healing Assay

The cells were cultured in six-well culture plates for 24 h and then "wounding" was induced by scratching directly using a sterilized pipette tip. After gentle washing with D-Hanks solution, the cells were cultured in Roswell Park Memorial Institute (RPMI)-1640 medium containing 1% FBS. Images of at least three randomly selected areas were captured using an Olympus digital camera at 0 and 24 h after the wounding.

RNA Fluorescence in situ Hybridization (FISH)

The RNA fluorescent in situ hybridization (FISH) was performed using a kit (C10910, RiboBio) according to the manufacturer's instructions. Biotin-labeled probes targeting circLRCH3 (Table 1) were synthesized by RiboBio Technology Co. Ltd. Fluorescence excitation was recorded using a Zeiss confocal laser scanning microscope (LSM 880 with Airyscan, Carl Zeiss).

Flow Cytometry

Flow cytometry was used to analyze the apoptotic CRC cells and their cell cycle distribution according to a previously described method.[26]

In vivo Animal Study

Male BALB/c nude mice (5 weeks old) were purchased from Beijing Vital River Laboratory Animal Technology Co., Ltd., and maintained under sterile specific pathogen-free conditions. LoVo cells (5×10^6 cells) from each group (n = 5 mice/group) were subcutaneously injected into the nude mice. Every 5 days, we measured the longitudinal and latitudinal diameters (L and d, respectively) of the tumor using calipers and the tumor volume was calculated using the following formula: V = 0.5 × L × W2 (W, width). After 25 days, the mice were euthanized and tumor tissues were weighed. All animal experiments were carried out in accordance with NIH Guidelines for the Care and Use of Laboratory Animals and approved by the Animal Care Committee of Tongji Medical College, Huazhong University of Science and Technology.

Statistical Analysis

We used the GraphPad Prism 6.0 software program to conduct the statistical analysis and all the data was expressed as means ± standard deviation. We performed a one-way analysis of variance (ANOVA) and Student's t-test to compare multiple or two groups, respectively to determine the statistical significance. A p-value < 0.05 was considered statistically significant.

Results

Screening and Characterization of circLRCH3 in CRC

To explore potential circRNAs that may play an important role in the progression of CRC, we downloaded two circRNA datasets related to CRC from the GEO database. Then, we calculated the DECs, determined the intersection, and identified four circRNAs with abnormal expression (Figure 1A–C). We designed divergent primers a the PCR analysis of four circRNAs showed that only hsa_circ_0008106 (renamed circLRCH3 as it derives from the pre-mRNA of LRCH3) primers ran out of products, consistent with the theory (Figure 1D) that this primer could not run out products of the gDNA. However, the corresponding convergent primers did run out of both cDNA and gDNA products, which confirmed the circular structure of this circRNA (Figure 1E).

The looping structure makes circRNAs more stable than linear RNAs, rendering them resistant to RNAse R (Figure 1F). Therefore, this circRNA, named circLRCH3, was selected for further analysis. Moreover, our exploration of circLRCH3 expression levels in CRC cells (Figure 1G) and tissues (Figure 1H, Table S1) showed it was down-regulated, which was consistent with GSE172229 and GSE138589. SW480 and LoVo cells, which expressed the lowest circLRCH3 levels were used for follow-up investigation. The RNA-FISH assay findings suggested the endogenous nuclear enrichment of circLRCH3 in CRC (Figure 1I).

circLRCH3 Overexpression Inhibits Proliferation, Invasion, and Migration of CRC Cells

To test the hypothesis that circLRCH3 serves as a tumor suppressor in CRC development and progression, we constructed circLRCH3 overexpressing vectors in SW480 and LoVo cells, which showed a relatively low expression and high yield efficiency (Figure 2A). Moreover, we found that exogenous circLRCH3 overexpression had no significant effect on the maternal LRCH3 mRNA level in both cell lines (Figure 2A). Furthermore, the results illustrated in Figure 2B–H show that the proliferation, invasion, and migration of SW480 and LoVo CRC cells were distinctly decreased by overexpression of circLRCH3. In contrast, circLRCH3 overexpression clearly blocked the cell cycle and enhanced apoptosis of CRC cells (Figure 3A and B). The results of the subcutaneous xenograft model analysis showed that the tumor size and weight were decreased in the circLRCH3 overexpression group (Figure 3C–E).

circLRCH3 Binds to oncomiRs miR-223

The miRNAs that bind to circLRCH3 were identified in the CircInteractome database. Two candidate miRNAs were obtained by overlapping predicted targeted miRNAs with DEMs and OS-related miRNAs (Figure 4A). Subsequently, only miR-223 showed a significant response to circLRCH3 upregulation (Figure 4B). The results showed that ectopic expression of miR-223 via mimic transfection only decreased the luciferase activity of report vectors expressing WT but
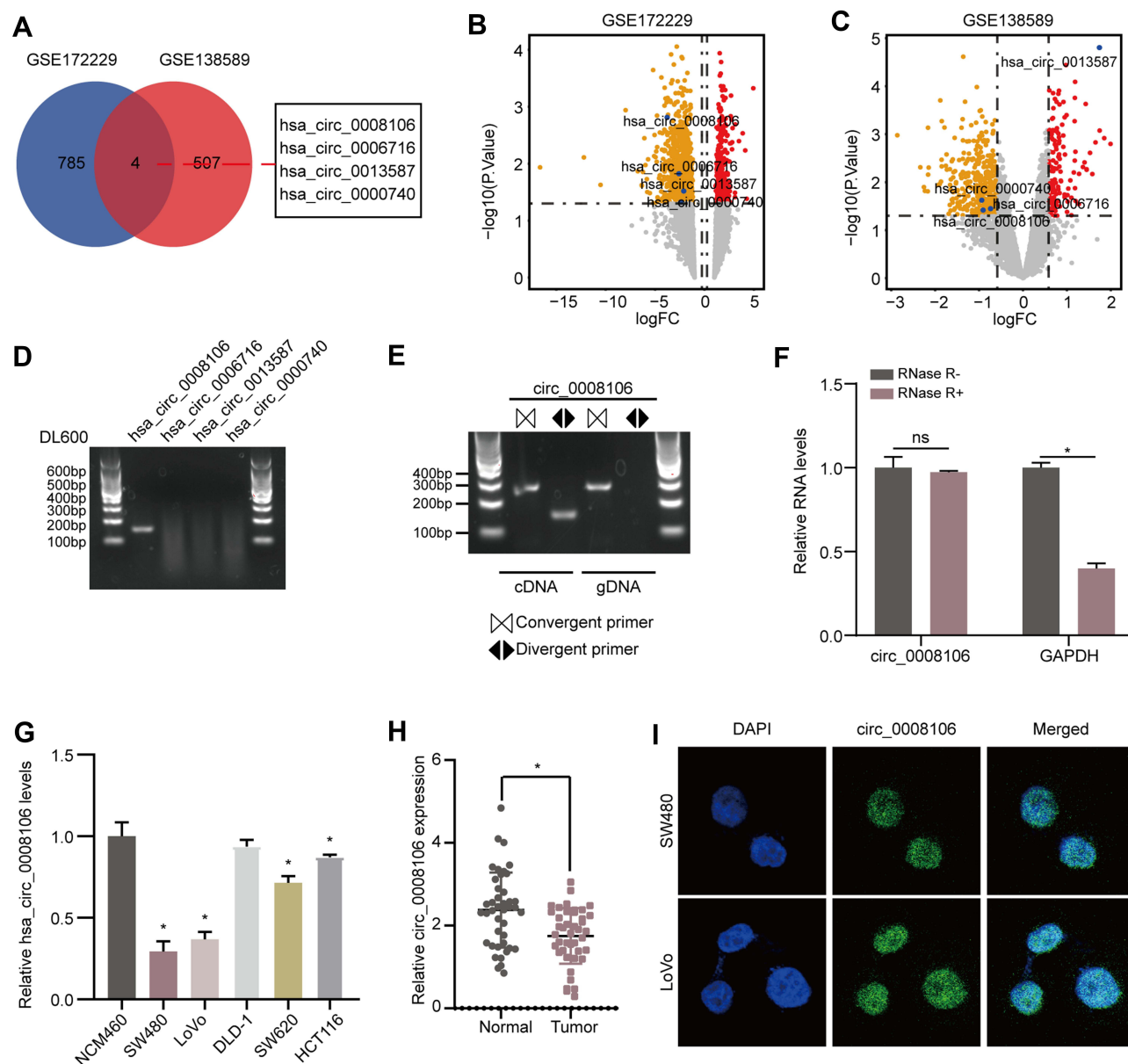
Figure 1 circLRCH3 is downregulated in CRC and characteristics of circLRCH3. (**A**) Overlapping analysis between GSE172229 and GSE138589. (**B** and **C**) The volcano plot of the four DECs in GSE172229 and GSE138589 datasets, respectively. (**D**) RT-PCR assay with divergent primers showing the detectable and undetectable circRNAs in cultured SW480 cells. (**E**) RT-PCR products using divergent and convergent primers indicating circularization of circLRCH3. cDNA represents complementary DNA. gDNA represents genomic DNA (right). (**F**) RT–qPCR assays were used to assess the expression of circLRCH3 and GAPDH mRNA in SW480 cells after treatment using RNase R. (**G**) RT-qPCR assay for the circLRCH3 in SW480, LoVo, DLD-1, SW620, HCT-116 and NCM460 cells. (**H**) RT-qPCR analysis of circLRCH3 in 46 CRC and NC samples. (**I**) The RNA-FISH assay revealed the nuclear localization of circLRCH3 in SW480 and LoVo cells by an antisense probe (green). Nuclei were stained with DAPI. *P<0.05. **Abbreviation**: ns, no significance.

not MUT-circLRCH3 in the CRC cells (Figure 4C and D). Furthermore, miR-223 showed a high expression level in both CRC cells and tissues (Figure 4E and F, Table S1) and high expression of miR-223 is associated with poor prognosis (Figure 4G). In addition, the attenuated proliferation, invasion, and migration of CRC cells by the circLRCH3 vector was restored by miR-223 mimics (Figure 4H–M).

LPP is Direct Target of miR-223 in CRC Cells

The assessment of the potential function of circLRCH3/miR-223 axis in CRC cells and exploration of potential miR-223 targets yielded seven consensus target genes (Figure 5A). The volcano plot analysis of the GSE156355 set and
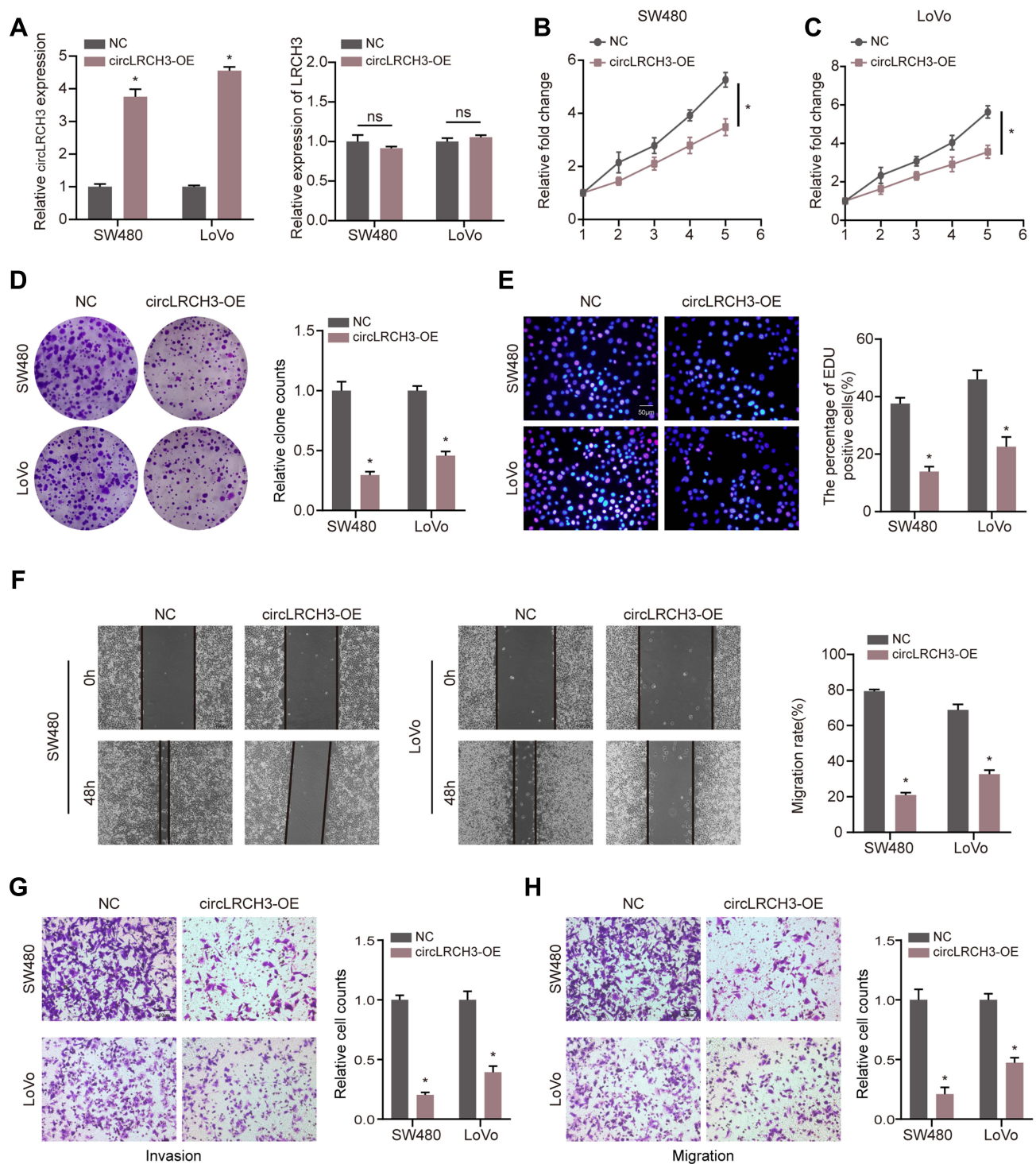
Figure 2 circLRCH3 inhibits the proliferation, invasion and migration of CRC cells. (**A**) Expression level of circLRCH3 was detected via RT-qPCR when the CRC cells were transfected with circLRCH3-OE vector and NC vector (left). The effect of circLRCH3 on LRCH3 mRNA expression level (right). (**B–H**) Influence of circLRCH3 on proliferation, invasion and migration of CRC cells based on MTT (**B** and **C**), colony formation (**D**), EdU (**E**), wound healing (**F**) and transwell assay (**G** and **H**). *P<0.05. **Abbreviation**: ns, no significance.

GSE50117 set (Figure 5B and C, respectively) identified seven DEGs, and LPP levels were dramatically lower in SW480 and LoVo cells than in NCM460 cells (Figure 5D). Similar results were obtained in CRC and normal tissues (Figure 5E).

Additionally, our Western blot analysis result indicated that increased miR-223 levels significantly reduced the expression of LPP in both CRC cell lines (Figure 5F). The miRWalk2.0 prediction showed complementarity between
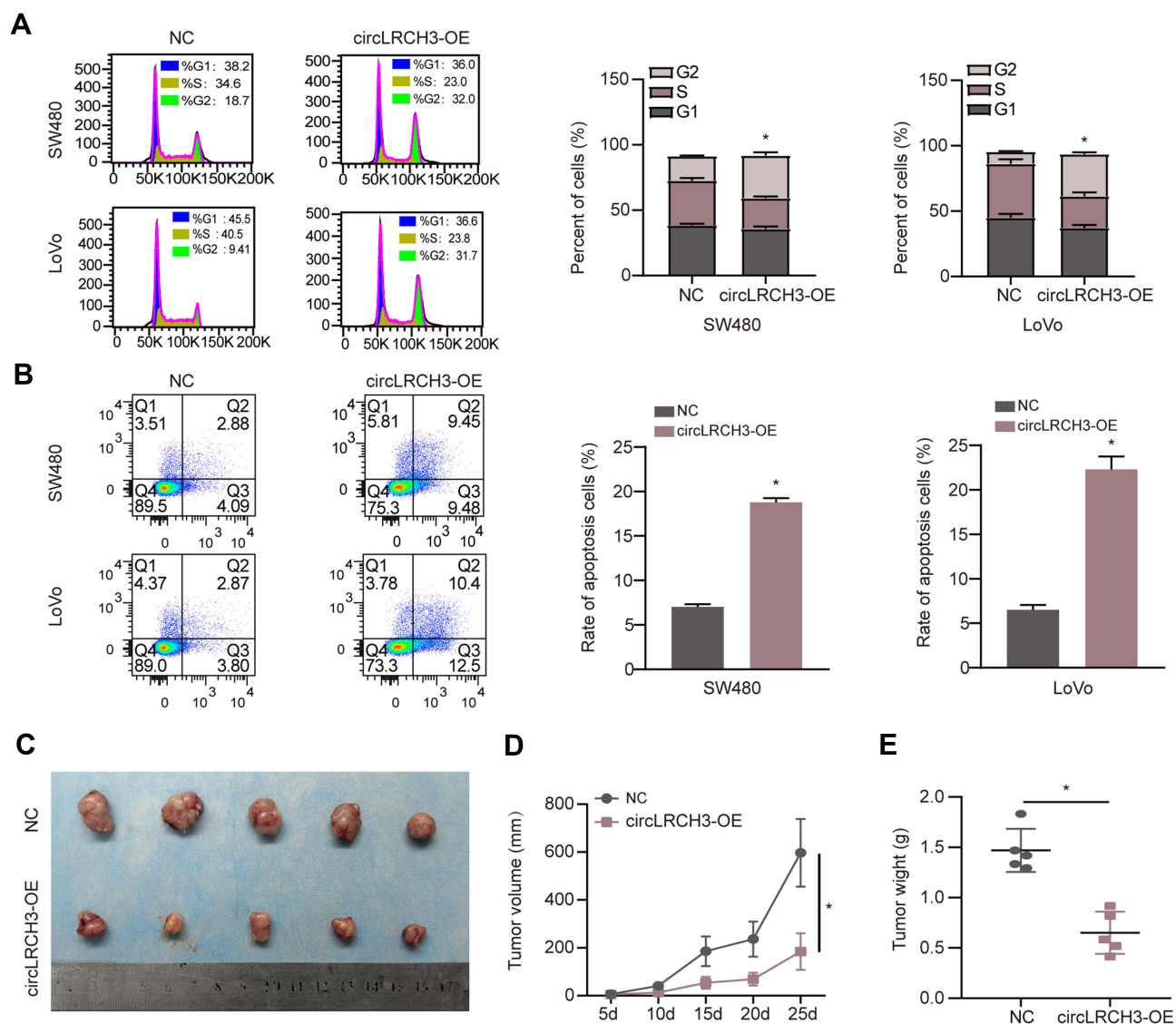
Figure 3 Effects of circLRCH3 on cell cycle and apoptosis and xenograft model in vivo. (**A** and **B**) The effect of circLRCH3 on the distribution of CRC cell cycle and apoptosis were assessed via flow cytometry. (**C–E**) In vivo growth curve (**D**) and weight at the end points (**E**) of xenografts formed by subcutaneous injection of SW480 cells stably transfected with mock, circLRCH3 into the dorsal flanks of nude mice (n=5 for each group). *P<0.05.
**Abbreviation**: ns, no significance.

miR-223 and the 3′UTR region of LPP (Figure 5G). The luciferase assay results displayed in Figure 5H showed that the relative activity of the WT reporter containing 3′UTR but not the mutant reporter was obviously suppressed in cells co-transfected with the miR-223 mimic.

circLRCH3 Promotes CRC Progression by Regulating LPP

The lentivirus-circLRCH3 and shRNA targeting LPP (sh-LPP) were co-transfected into CRC cells to verify the effect of LPP on proliferation, invasion, and migration of circLRCH3 overexpressing CRC cells. Knockdown of LPP was verified using RT-qPCR and Western blot analysis (Figure 6A and B). As demonstrated by the results shown in Figure 6C–E, overexpression of circLRCH3 reversed the promotion of CRC cell proliferation, invasion, and migration ability by LPP knockdown.
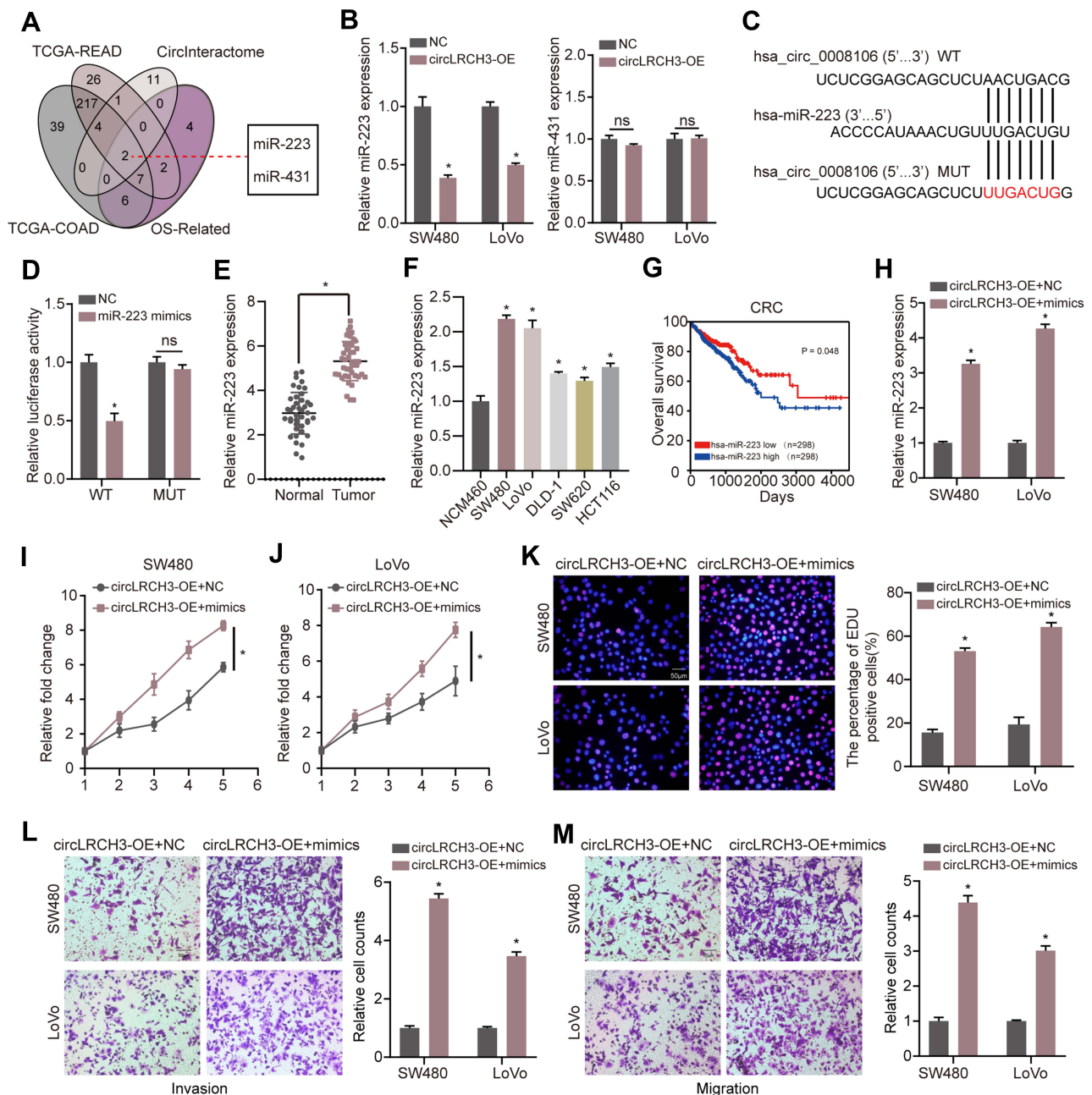
Figure 4 MiR-223 sponges circLRCH3 and could rescue the anti-tumor effect of circLRCH3 on CRC cells. (**A**) Venn diagram of the miRNAs from TCGA-READ and TCGA-COAD with CircInteractome predicted targets and OS-related miRNAs. (**B**) The effect of circLRCH3 on the expression of miR-223 and miR-413. (**C** and **D**) pMIR-REPORT luciferase vector containing WT-circLRCH3 or a mutated type was co-transfected in SW480 cells with miR-223 mimics or miR-NC. Firefly luciferase activity was measured according to Renilla luciferase activity. (**E** and **F**) RT-qPCR was applied to measure the expression level of miR-223 in CRC tissues and cells.(**G**) Kaplan-Meier analysis was used to determine overall survival of patients with miR-223 high or low expression from TCGA database . (**H**) RT-qPCR was used to assess the expression level of miR-223 in circLRCH3-overexpression cells transfected with miR-223 mimics. (**I–M**) The effect of miR-223 on proliferation, invasion and migration of circLRCH3-overexpression CRC cells. *P<0.05.
Abbreviation: ns, no significance.

Discussion

In the present study, we extracted circRNA microarray data from the GEO database with circLRCH3 as the main molecule of interest among DECs in CRC. The effects of circLRCH3 has not been widely reported in tumors and needs to be confirmed through relevant experiments. We performed several validation assays to verify the circular structure of the circLRCH3, which ruled out the possibility of genome rearrangement or trans-splicing, Furthermore, the results were
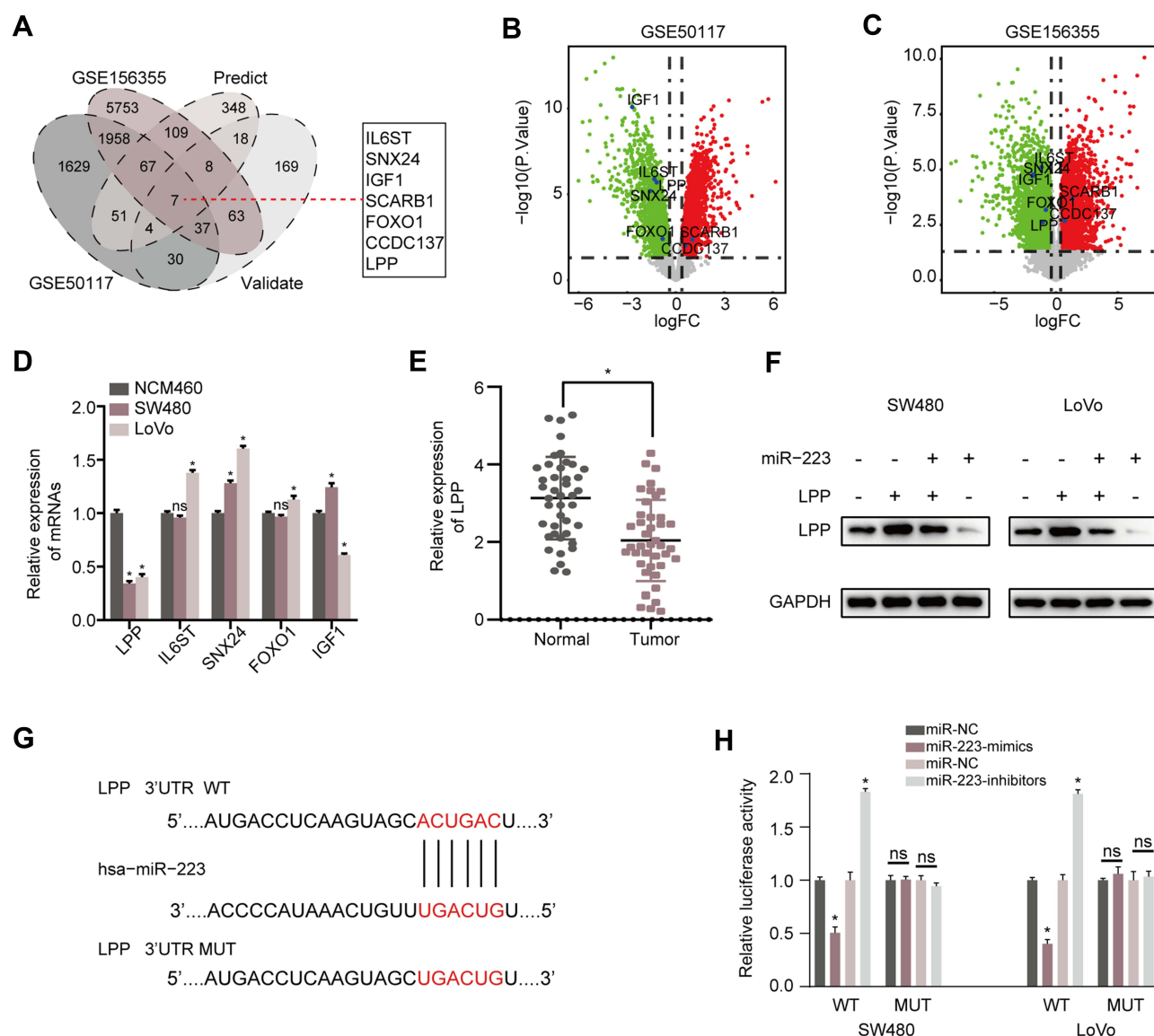
Figure 5 LPP is a direct target of miR-223 in CRC cells. (**A**) Venn diagram of the DEGs from GSE156355 and GSE50117 with predicted targets and validated targets. (**B** and **C**) Volcano plot of the selected seven DEGs in GSE156355 and GSE50117 sets, respectively. (**D**) RT-qPCR analysis for the identified consensus five DEGs in SW480, LoVo and NCM460 cells. (**E**) RT-qPCR was applied to measure the expression level of LPP mRNA in CRC tissues. (**F**) The effect of miR-223 on the protein level of LPP in CRC cells. (**G**) The key binding site of the LPP mRNA 3'-UTR for miR-223. (**H**) pMIR-REPORT luciferase vector containing LPP 3'UTR or a mutated type was co-transfected in SW480 and LoVo cells with miR-223 mimics or inhibitors or miR-NC. Firefly luciferase activity was measured according to Renilla luciferase activity. *P<0.05.
Abbreviation: ns, no significance.

consistent with those previously reported in canonical literature on circRNA.[27,28] To the best of our knowledge, this is the first study to show that circLRCH3 is a tumor suppressor in CRC, experiments showing that its downregulation in CRC cells contributed to CRC progression and metastasis. Furthermore, the downregulation of circLRCH3 in CRC cells led us to hypothesize that circLRCH3 served as a tumor suppressor in CRC development and progression.

CircRNA has been reported to be generated from encoding genes and regulate its parent genes in a cis-acting manner.[29,30] CircLRCH3 is derived from LRCH3, but we found that it has no regulatory effect on LRCH3. This result indicated that circLRCH3 exerts its CRC tumor suppression through other mechanisms. CircRNA regulates gene expression by sponging miRNAs, which is an important regulatory mechanism. These results showed that circLRCH3 might function as an miR-223 sponge in CRC cells through target binding. CircRNA regulates gene levels by binding miRNA and blocking its inhibition of target genes, thereby participating in tumorigenesis.[31]

A

B

C

D

E
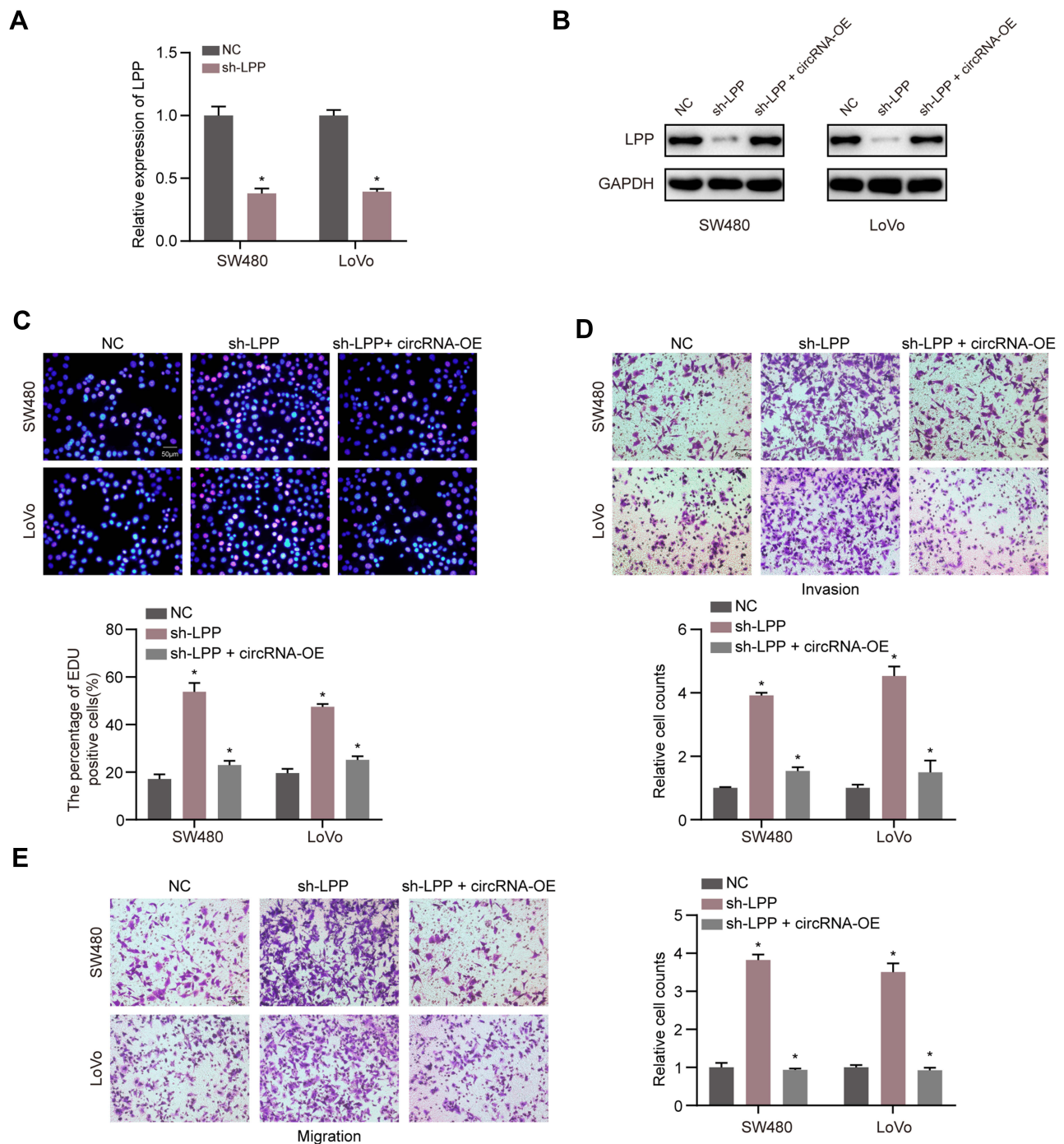
Figure 6 The anti-tumor effect of LPP could be reversed by circLRCH3. (**A**) Expression level of LPP mRNA level was detected via RT-qPCR when the CRC cells were transfected with sh-LPP vector and NC vector. (**B**) The LPP protein level was measured by Western blot after transfection of sh-LPP vector, sh-LPP + circLRCH3-OE vector and NC vector. (**C–E**) The effect of circLRCH3 and LPP on the proliferation (**C**) invasion (**D**) and migration (**E**) of SW480 and LoVo cells. *P<0.05.
Abbreviation: ns, no significance.

We found that circLRCH3 binds miR-223 and inhibits its functions. MiR-223 has been revealed to be associated with various kinds of cancers. Nevertheless, current studies are controversial and it is unclear whether miR-223 suppresses or promotes cancer development. For instance, Tang et al reported that miR-223 inhibited metastasis of human cervical cancer through modulating epithelial-mesenchymal transition.[32] Furthermore, another study reported that miR-223 was more overexpressed in pancreatic cancer patients than it was in age-matched healthy individuals.[33] A possible

explanation for this discrepancy is that miR-223 can be differentially expressed in different cancer cell types. The mechanism underlying miR-223 dysregulation in CRC has still not been fully clarified. In this study, we elucidated a novel mechanism underlying miR-223 regulation, where its regulation of other genes is weakened following absorption on circLRCH3. We further revealed that downregulation of circLRCH3 in CRC dysregulated miR-223 and its targets, highlighting the important regulatory role of circLRCH3 on miR-223.

In our study, the expression level of circLRCH3 was found to significantly correlated with several clinicopathologic indicators, including tumor size and tumor, nodal, and metastasis (TNM) stage in our CRC cohort. These results suggest that circLRCH3 may serve as a novel diagnostic and therapeutic target for CRC. The results also showed that the experimental CRC cell lines had higher miR-223 levels than those of the human colorectal cell lines. The Kaplan–Meier survival analysis showed that a high level of miR-223 was associated with a poor OS, indicating that miR-223 may act as a marker for poor prognosis of CRC patients. The MTT and transwell assays to further explore the role of miR-223 in CRC showed that its overexpression promoted the proliferation, invasion, and migration of CRC cells, which was reversed by circLRCH3. These findings also indicate that upregulation of circLRCH3 expression in CRC cells could inhibit CRC progression. In addition, downregulation of LPP expression enhanced CRC cell proliferation, invasion, and migration, which was effectively reverted by miR-223 inhibitors or circLRCH3 upregulation. These results indicate that the combination of these three molecules could be used as a biomarker to aid clinical diagnosis and a combination of multiple molecular interventions to treat CRC is promising.

An increasing number of studies suggest that miRNAs play critical roles in tumorigenesis. For instance, Tian et al suggested that upregulation of miRNA-154-5p prevented the tumorigenesis of osteosarcoma.[34] Xie et al reported that deep RNA sequencing revealed the dynamic regulation of miRNA, lncRNAs, and mRNAs in osteosarcoma tumorigenesis and pulmonary metastasis.[35] Qu et al indicated that miRNA-558 promoted tumorigenesis and aggressiveness of neuroblastoma cells by activating the transcription of heparanase.[36] Importantly, numerous studies have reported the usefulness of miRNA in the treatment of various cancers. For instance, Lindholm et al reported miRNA expression changes during neoadjuvant bevacizumab and chemotherapy treatment of breast cancer.[37] In addition, Rodríguez-Martínez et al identified exosomal miRNA profiles as a complementary tool in the diagnosis and prediction of treatment responses in localized breast cancer patients under neoadjuvant chemotherapy.[38] Xiao et al constructed a circRNA-miRNA-mRNA network to analyze the pathogenesis and treatment of pancreatic ductal adenocarcinoma;[39] however whereas the role of miR-223 in CRC remains poorly understood. We found that miR-223 was elevated in CRC patients using bioinformatics methods, which demonstrated that miR-223 may act as an oncogenic miRNA in CRC development. In the present study, we investigated miR-223 expression in CRC tissue and corresponding non-tumor tissues. Results discovered that the expression of miR-223 was obviously increased in CRC tissues compared with that in non-tumor tissues. The levels of miR-223 were also assessed in the two CRC cell lines. The results showed that the CRC cell lines had higher miR-223 levels than human colorectal cell line. The Kaplan–Meier survival analysis showed that a high miR-223 level was associated with a poor OS, indicating that miR-223 may act as a marker for poor prognosis of CRC. To further explore the role of miR-223 in CRC, miR-223 mimics were transfected into CRC cells and the subsequent MTT assay results indicated that miR-223 overexpression promoted the proliferation of PC cells. Moreover, the transwell assay results suggested that miR-223 overexpression enhanced invasion and migration of PC cells. The result of the flow cytometry showed that miR-223 overexpression enhanced the CRC cell cycle and inhibited their apoptosis. These results suggest that miR-223 may serve as an oncogene in CRC.

To better understand the molecular mechanism by which miR-223 functions as an oncogene in CRC, target genes of miR-223, such as LPP, were explored. LPP has reported to act as tumor suppressor in lung cancer.[40] However, no relevant study has explored the biological effect of LPP in CRC and the relationship between circLRCH3 and LPP. In this study, the bioinformatic analysis confirmed *LPP* as a new direct target gene of miR-223, whereas the luciferase reporter assay suggested that miR-223 directly targeted the 3′-UTR of LPP.

In addition, the rescue study results indicated that LPP overexpression repressed CRC proliferation, invasion, and migration, which was effectively reversed by miR-223 overexpression. These results corroborated the findings of the luciferase assay, which showed that miR-223 directly regulated the gene expression via binding sequence at the 3′UTR of LPP. We speculated that miR-223 might function in CRC cells through the direct downregulation of LPP. These results

indicate that miR-223 has a tumor-promoting role in CRC carcinogenesis and progression mediated through the negative regulation of LPP expression. This finding indicates that miR-223-based targeted treatment could be a novel therapeutic target for CRC patients.

In addition, a previous study found that LPP inhibited collective cell migration during lung cancer dissemination,[40] which is consistent with the result of our study. Taken together, these findings indicate that miR-223 might target the LPP mRNA to enhance the proliferation of CRC, and circLRCH3 might regulate LPP by sponging miR-223.

Conclusion

Our findings indicated that circLRCH3 inhibits proliferation, migration, and invasion of colorectal cancer cells through miRNA-223/LPP axis. The findings of this study provide novel insights into the mechanisms underlying the development and metastasis of CRC, whereas, the details of the potential mechanism remained to be explored further.

Data Sharing Statement

The data that support the findings of this study are available from the corresponding author upon reasonable request.

Acknowledgment

The authors sincerely appreciate all lab members.

Funding

Disclosure

The authors report no conflicts of interest in this work.

References

1. Bray F, Ferlay J, Soerjomataram I, Siegel RL, Torre LA, Jemal A. Global cancer statistics 2018: GLOBOCAN estimates of incidence and mortality worldwide for 36 cancers in 185 countries. *CA Cancer J Clin*. 2018;68(6):394–424. doi:10.3322/caac.21492
2. Ferlay J, Colombet M, Soerjomataram I, et al. Estimating the global cancer incidence and mortality in 2018: GLOBOCAN sources and methods. *Int J Cancer*. 2019;144(8):1941–1953. doi:10.1002/ijc.31937
3. Arnold M, Sierra MS, Laversanne M, Soerjomataram I, Jemal A, Bray F. Global patterns and trends in colorectal cancer incidence and mortality. *Gut*. 2017;66(4):683–691. doi:10.1136/gutjnl-2015-310912
4. Franke AJ, Parekh H, Starr JS, Tan SA, Iqbal A, George TJ Jr. Total neoadjuvant therapy: a shifting paradigm in locally advanced rectal cancer management. *Clin Colorectal Cancer*. 2018;17(1):1–12. doi:10.1016/j.clcc.2017.06.008
5. Sung JJY, Chiu HM, Jung KW, et al. Increasing trend in young-onset colorectal cancer in Asia: more cancers in men and more rectal cancers. *Am J Gastroenterol*. 2019;114(2):322–329. doi:10.14309/ajg.0000000000000133
6. Jeck WR, Sharpless NE. Detecting and characterizing circular RNAs. *Nat Biotechnol*. 2014;32(5):453–461. doi:10.1038/nbt.2890
7. Li X, Yang L, Chen LL, Biogenesis T. Functions, and challenges of circular RNAs. *Mol Cell*. 2018;71(3):428–442. doi:10.1016/j.molcel.2018.06.034
8. Kristensen LS, Andersen MS, Stagsted LVW, Ebbesen KK, Hansen TB, Kjems J. The biogenesis, biology and characterization of circular RNAs. *Nat Rev Genet*. 2019;20(11):675–691. doi:10.1038/s41576-019-0158-7
9. Li P, Song R, Yin F, et al. circMRPS35 promotes malignant progression and cisplatin resistance in hepatocellular carcinoma. *Mol Ther*. 2022;30(1):431–447. doi:10.1016/j.ymthe.2021.08.027
10. Yang F, Fang E, Mei H, et al. Cis-acting circ-CTNNB1 promotes beta-catenin signaling and cancer progression via DDX3-mediated transactivation of YY1. *Cancer Res*. 2019;79(3):557–571. doi:10.1158/0008-5472.CAN-18-1559
11. Gao X, Xia X, Li F, et al. Circular RNA-encoded oncogenic E-cadherin variant promotes glioblastoma tumorigenicity through activation of EGFR-STAT3 signalling. *Nat Cell Biol*. 2021;23(3):278–291. doi:10.1038/s41556-021-00639-4
12. Esquela-Kerscher A, Slack FJ. Oncomirs - microRNAs with a role in cancer. *Nat Rev Cancer*. 2006;6(4):259–269. doi:10.1038/nrc1840
13. Croce CM. Causes and consequences of microRNA dysregulation in cancer. *Nat Rev Genet*. 2009;10(10):704–714. doi:10.1038/nrg2634
14. Pauli A, Rinn JL, Schier AF. Non-coding RNAs as regulators of embryogenesis. *Nat Rev Genet*. 2011;12(2):136–149. doi:10.1038/nrg2904
15. Qu H, Zhu F, Dong H, Hu X, Han M. Upregulation of CCT-3 induces breast cancer cell proliferation through miR-223 competition and Wnt/beta-catenin signaling pathway activation. *Front Oncol*. 2020;10:533176. doi:10.3389/fonc.2020.533176
16. Dong X, Kong C, Liu X, et al. GAS5 functions as a ceRNA to regulate hZIP1 expression by sponging miR-223 in clear cell renal cell carcinoma. *Am J Cancer Res*. 2018;8(8):1414–1426.

17. Petit MM, Mols R, Schoenmakers EF, Mandahl N, Van de Ven WJM. LPP, the preferred fusion partner gene of HMGIC in lipomas, is a novel member of the LIM protein gene family. *Genomics*. 1996;36(1):118–129. doi:10.1006/geno.1996.0432

18. Diboun I, Wernisch L, Orengo CA, Koltzenburg M. Microarray analysis after RNA amplification can detect pronounced differences in gene expression using limma. *BMC Genomics*. 2006;7:252. doi:10.1186/1471-2164-7-252

19. Varet H, Brillet-Guéguen L, Coppée JY, Dillies MA. SARTools: a DESeq2- and EdgeR-based R pipeline for comprehensive differential analysis of RNA-seq data. *PLoS One*. 2016;11(6):e0157022. doi:10.1371/journal.pone.0157022

20. Glazar P, Papavasileiou P, Rajewsky N. circBase: a database for circular RNAs. *RNA*. 2014;20(11):1666–1670. doi:10.1261/rna.043687.113

21. Dudekula DB, Panda AC, Grammatikakis I, De S, Abdelmohsen K, Gorospe M. CircInteractome: a web tool for exploring circular RNAs and their interacting proteins and microRNAs. *RNA Biol*. 2016;13(1):34–42. doi:10.1080/15476286.2015.1128065

22. Dweep H, Gretz N, Sticht C. miRWalk database for miRNA-target interactions. *Methods Mol Biol*. 2014;1182:289–305.

23. Friedman RC, Farh KK, Burge CB, Bartel DP. Most mammalian mRNAs are conserved targets of microRNAs. *Genome Res*. 2009;19(1):92–105. doi:10.1101/gr.082701.108

24. Betel D, Koppal A, Agius P, Sander C, Leslie C. Comprehensive modeling of microRNA targets predicts functional non-conserved and non-canonical sites. *Genome Biol*. 2010;11(8):R90. doi:10.1186/gb-2010-11-8-r90

25. Kertesz M, Iovino N, Unnerstall U, Gaul U, Segal E. The role of site accessibility in microRNA target recognition. *Nat Genet*. 2007;39(10):1278–1284. doi:10.1038/ng2135

26. Xu Y, Zhang X, Hu X, et al. The effects of lncRNA MALAT1 on proliferation, invasion and migration in colorectal cancer through regulating SOX9. *Mol Med*. 2018;24(1):52. doi:10.1186/s10020-018-0050-5

27. Memczak S, Jens M, Elefsinioti A, et al. Circular RNAs are a large class of animal RNAs with regulatory potency. *Nature*. 2013;495(7441):333–338. doi:10.1038/nature11928

28. Piwecka M, Glazar P, Hernandez-Miranda LR, et al. Loss of a mammalian circular RNA locus causes miRNA deregulation and affects brain function. *Science*. 2017;357:6357. doi:10.1126/science.aam8526

29. Yao Z, Luo J, Hu K, et al. ZKSCAN1 gene and its related circular RNA (circZKSCAN1) both inhibit hepatocellular carcinoma cell growth, migration, and invasion but through different signaling pathways. *Mol Oncol*. 2017;11(4):422–437. doi:10.1002/1878-0261.12045

30. Liang WC, Wong CW, Liang PP, et al. Translation of the circular RNA circbeta-catenin promotes liver cancer cell growth through activation of the Wnt pathway. *Genome Biol*. 2019;20(1):84. doi:10.1186/s13059-019-1685-4

31. Li J, Sun D, Pu W, Wang J, Circular PY. RNAs in cancer: biogenesis, function, and clinical significance. *Trends Cancer*. 2020;6(4):319–336. doi:10.1016/j.trecan.2020.01.012

32. Tang Y, Wang Y, Chen Q, Qiu N, Zhao Y, You X. MiR-223 inhibited cell metastasis of human cervical cancer by modulating epithelial-mesenchymal transition. *Int J Clin Exp Pathol*. 2015;8(9):11224–11229.

33. Debernardi S, Massat NJ, Radon TP, et al. Noninvasive urinary miRNA biomarkers for early detection of pancreatic adenocarcinoma. *Am J Cancer Res*. 2015;5(11):3455–3466.

34. Tian Q, Gu Y, Wang F, et al. Upregulation of miRNA-154-5p prevents the tumorigenesis of osteosarcoma. *Biomed Pharmacother*. 2020;124:109884. doi:10.1016/j.biopha.2020.109884

35. Xie L, Yao Z, Zhang Y, et al. Deep RNA sequencing reveals the dynamic regulation of miRNA, lncRNAs, and mRNAs in osteosarcoma tumorigenesis and pulmonary metastasis. *Cell Death Dis*. 2018;9(7):772. doi:10.1038/s41419-018-0813-5

36. Qu H, Zheng L, Pu J, et al. miRNA-558 promotes tumorigenesis and aggressiveness of neuroblastoma cells through activating the transcription of heparanase. *Hum Mol Genet*. 2015;24(9):2539–2551. doi:10.1093/hmg/ddv018

37. Lindholm EM, Ragle Aure M, Haugen MH, et al. miRNA expression changes during the course of neoadjuvant bevacizumab and chemotherapy treatment in breast cancer. *Mol Oncol*. 2019;13(10):2278–2296. doi:10.1002/1878-0261.12561

38. Rodríguez-Martínez A, de Miguel-Pérez D, Ortega FG, et al. Exosomal miRNA profile as complementary tool in the diagnostic and prediction of treatment response in localized breast cancer under neoadjuvant chemotherapy. *Breast Cancer Res*. 2019;21(1):21. doi:10.1186/s13058-019-1109-0

39. Xiao Y. Construction of a circRNA-miRNA-mRNA network to explore the pathogenesis and treatment of pancreatic ductal adenocarcinoma. *J Cell Biochem*. 2020;121(1):394–406. doi:10.1002/jcb.29194

40. Kuriyama S, Yoshida M, Yano S, et al. LPP inhibits collective cell migration during lung cancer dissemination. *Oncogene*. 2016;35(8):952–964. doi:10.1038/onc.2015.155